Interferometric closed-loop fiber-optic gyroscopes

Yuri N. Korkishko, Vyacheslav A. Fedorov, Victor E. Prilutskii, Vladimir G. Ponomarev,
Ivan V.Morev, Sergey M.Kostritskii
RPC Optolink, Ltd., Moscow 124498, Zelenograd, proezd 4806, h.5, Russia

ABSTRACT

The operation of Fiber Optic Gyro is based on the Sagnac Effect which states that light beams propagating along opposite directions in a rotating frame experience an optical path length difference. These two counter-propagating waves propagate within a closed fiber coil, and when this coil rotates the resultant phase difference is proportional to the rotation rate Ω. Fiber optic gyroscopes are desirable devices for many navigation and guidance applications because, being solid state devices, they have several major advantages including light weight, long working lifetimes, no moving parts and operate using low voltage power. In this paper the Optolink's single-axis and three-axis fiber optic gyroscopes are described. The Optolink's FOGs consist of the light-emitting diode, one or three photodetectors, circulators and polarization maintaining fiber couplers to divide the light into two or three parts, one or three sets of ring interferometers to sense one or three orthogonal angular rates, and installed PCB signal processing circuits. The ring interferometer consists of a multifunction integrated optic chip and polarization maintaining fiber coil, both these components are designed and fabricated by Optolink. The results illustrate the versatility of the technology, showing its potential to meet both the low-cost, compact sized needs of tactical guidance, as well as the very high performance needs of inertial navigation and precision applications. The optic and electronic blocks of closed-loop gyroscopes with integrated optic components are also considered in this paper.

1. INTRODUCTION

Over the last twenty years, the interferometric fiber-optic gyroscope (FOG) has evolved from pioneering physics experiment to a practical device that is now in production. Today, it is now accepted among inertial guidance and navigation specialists that FOG is a strong contender for many civilian and military applications. FOGs are well known as sensors for rotation, which are based on Sagnac effect [1], and have been under development for a number of years to meet a wide range of performance requirements. As it is with ring laser gyroscope (RLG), FOG can be used for higher reliability and longer lifetime applications, as well as in more severe environment due to the absence of revolving components. Relative advantages of the FOG over the RLG are the lack of a high-voltage power supply requirement, the elimination of mechanical dither and associated with it reaction torques, and the ability to obtain small angle quantization more easily.

2. RESULTS

2.1 Configuration

Optolink Ltd. designed and started the industrial fabrication of the family of closed loop fiber-optic gyroscopes (FOG) the worked as a rotation rate sensor. Both 1-axis and 3-axis FOGs have been successfully developed. Our FOGs have so-called minimum configuration (Figs.1,3) that provides reciprocal optical paths for two counter-propagating beams in a fiber loop. The FOG consists of the one Light Source (SLD), one Photodetector, circulator (C) and PM Fiber Couplers to divide the light into two or three parts, one or three sets of ring interferometers to sense one or three orthogonal angular rate, and installed PCB signal processing circuits. The ring interferometer consists of a multifunction integrated optic chip (MIOC) and polarization maintaining (PM) fiber coil . The MIOC is a three-port optical gyrochip fabricated at lithium niobate wafer by high temperature proton exchange technique [2], and itprovides three functions. First, it polarizes the propagating light to reduce bias instability due to polarization non-reciprocity. Second, it splits the light into clockwise and counterclockwise waves, each with equal optical power, and recombines them with a Y-junction waveguide. Third, with electro-optical phase modulator, it applies a biasing phase shift to the counter-propagating

Third Asia Pacific Optical Sensors Conference, edited by John Canning, Gangding Peng,
Proc. of SPIE Vol. 8351, 83513L · © 2012 SPIE · CCC code: 0277-786X/12/$18 · doi: 10.1117/12.912937

beams. PM fiber is used in order to reduce both the drift caused by the polarization cross coupling and the drift caused by earth's and outside magnetic field via the Faraday effect. The SLD light source, supplied by DenseLight Corp. (Singapore) generates the light that would pass through circulator and splits evenly into two ways at the Y-junction of the MIOC. The two waves travel inside the fiber sensing coil in clockwise and counter-wise directions respectively, then interfere back at the Y-junction and arrive at the photodetector module through circulator. When the system is a subject of rotation, the two waves experience a phase difference because of the different optical path lengths:

$$\varphi_s = \frac{2\pi LD}{\lambda c}\Omega = \frac{2\pi^2 D^2 N}{\lambda \cdot c}\Omega$$

where L is the coil length, D- coil diameter, N- number of coil turnes, λ- is the wavelength in vacuum and c is the light speed.

Depending on sensitivity, bias drift and dynamic range, different types of Optolink's gyros contain from 200 m to 2000 m long fiber optical coil, made from self-produced single mode (at 1550) nm wavelength polarization maintaining (PM) fiber (PANDA type) with low optical loss ($\alpha < 2$ dB/km) and high polarization-holding parameter ($h \leq 10^{-5}$ m^{-1}). The fiber coils are fabricated by symmetrical winding with stable stretch. The coil is placed on a temperature isolated plate with diameter from 60 to 230 mm depending on type of FOG (see Table 1). PIN photodiodes (PD) are used as a receiver, and pigtailed temperature stabilized superluminescent diode (SLD) with output power from 10 to 20 mW is used as a light source. Stabilization of temperature of SLD by Pelletier module enables one to achieve temperature stability of FOG's scale factor. Our 3-Axis FOGs use just one light source for three fiber coils (Fig.3).

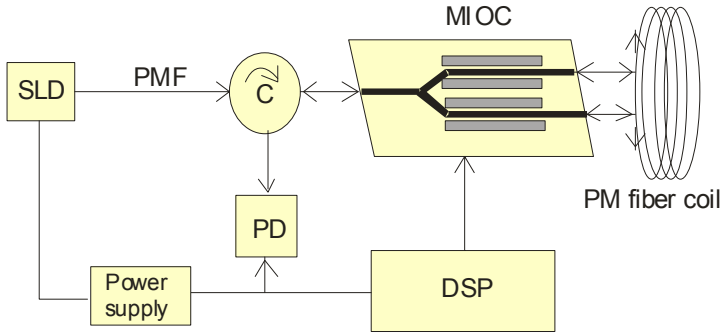

Fig.1. Single axis FOG configuration.

SRS-2000 **SRS-1000** **SRS-501** **SRS-200**

Fig.2. Single axis Optolink's FOGs.

The photos of single-axis and three-axis gyros are shown at Figs.2,4.

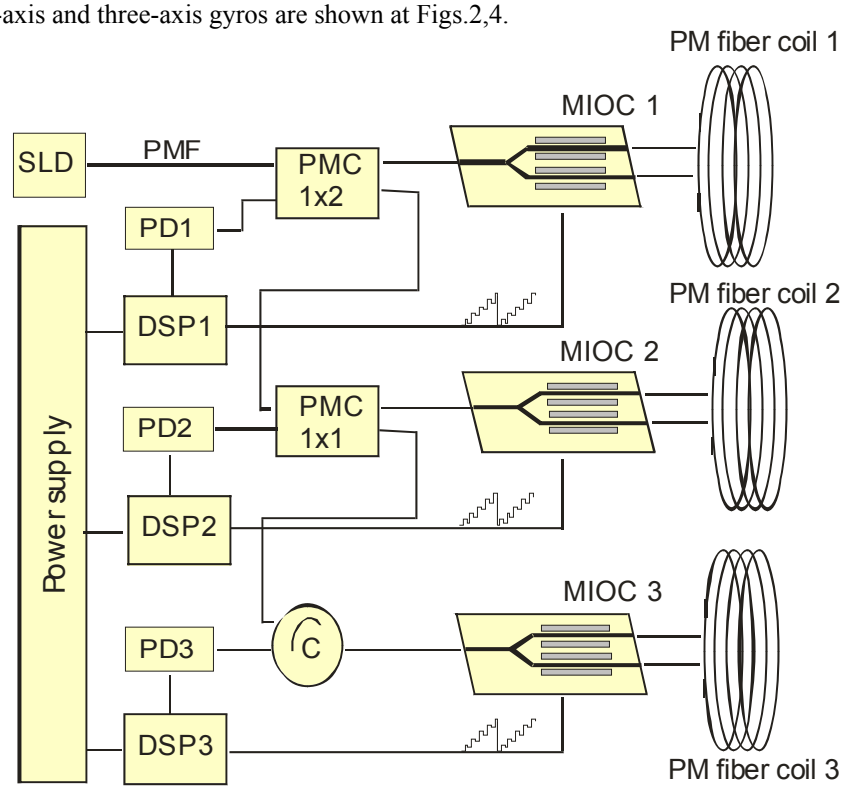

Fig.3. Three axis FOG configuration.

Fig.4. Three-axis Optolink's gyro TRS-500.

1.2. PM fiber

The accuracy of FOG depends strongly on parameters of optical block. The device noise is smaller the larger is output power of SLD and smaller optical losses at all optical components, including PM fiber. The minimal measured rotation rate depends on polarization crosstalk h and beat length L_p of PM fiber as following [3]:

$$\Omega_{\min} \sim \frac{\sqrt{hL_p}}{DL}$$

Thus, the main our activity was directed to reduce optical loss, polarization crosstalk and beat length in PANDA fibers. Table 1 shows the present parameters of Optolink's PM fibers.

Table 1. Parameters of Optolinks PM fibers.

Operating wavelength	1.55 μm
Mode Field Diameter	6.5 μm
Cladding Diameter	80 μm
Coating Diameter	120÷160 μm
Numerical Aperture	0.13
Polarization crosstalk (h-Parameter)	$<10^{-5}$ /m
Attenuation	< 2 dB/km
Cutoff Wavelength	1250nm-1450nm
Beat Length	<3mm
Stress Type	PANDA

Four families of single-axis FOGs having fiber coils with lengths 200 m (SRS-200), 500 m (SRS-500), 1000 m (SRS-1000) and 2000 m (SRS-2000) are developed. Quadrupole winding technique implies winding a coil from a single length of fiber, starting at the center of the fiber length, winding outward toward the ends, alternately from one or another of two supply spools, in a geometrically structured way. Indeed, optical fiber is elastic but very delicate. Elasticity implies a need to keep fiber always under constant tension during winding. Delicacy implies a need to control not only in-process fiber tension, but also fiber flexure or curvature, and a surface contacts. The coil is placed at the temperature isolated plate with diameter from 80 to 230 mm depending on type of FOG (see Table 2). Our fiber coil winding machine was specially developed on the basis of standard wire winding machine.

1.3. Integrated optical components

One of the main fiber-optic gyroscope components is a multifunctional integrated optical chip (MIOC). Optolink's MIOC is a solid state waveguide device on X-cut $LiNbO_3$ substrate fabricated by High-Temperature Proton Exchange method (HTPE) [2]. It includes a linear polarizer, Y-junction coupler and two pairs of electro-optic phase modulators. Light coming from the optical fiber coupler is linearly polarized within the MIOC to greater than 60 dB. This high degree of polarization minimizes bias uncertainty due to polarization non-reciprocity. The Y-junction coupler within the MIOC splits the light into equal amplitude waves, each directed along a separated waveguide within the MIOC. Each of the resulting waves pass through an electrooptical phase modulator, and after that two waves counterpropagate around the optical PM optical fiber sensor coil.

A very important advantage of proton exchange (PE) waveguides is the following. In such waveguides the extraordinary refraction index is increasing, while the refraction index of ordinary ray is decreasing. As a result, proton exchanged waveguides support the propagation of only extraordinary polarization modes (TE in our case). Therefore, there is no necessity to use a polarizer in the fiber-optic gyroscope, which brings additional loss.

It is well known that standard technology of PE waveguide (APE-technology) [4] is a two-level process, which consists of a PE, (melting pure or diluted by lithium benzoate benzoic acid as a rule) and subsequent annealing (Fig.5a). It has been recently obtained that different defects are formed in the surface area of a waveguide due to different phase transitions [5]. These defects are sources of additional scattering of light.

In paper [2] we reported the fabrication and characterization of $LiNbO_3$ optical waveguides prepared by HTPE process with a new proton exchange source, i.e., the mixture of stearic acid and lithium stearate. The melt used is characterized by the mass ratio of lithium stearate (LS) and stearic acid (SA): $\rho = m_{LS} / m_{SA}$. Varying ρ in range from 0 to 1% strongly

modifies the phase of the exchanged layer. HTPE process, in contrast to APE, is a one step process and does not allow any phase transitions (Fig.5) and, therefore, allows one to achieve the smaller optical losses and higher electro-optical coefficients.

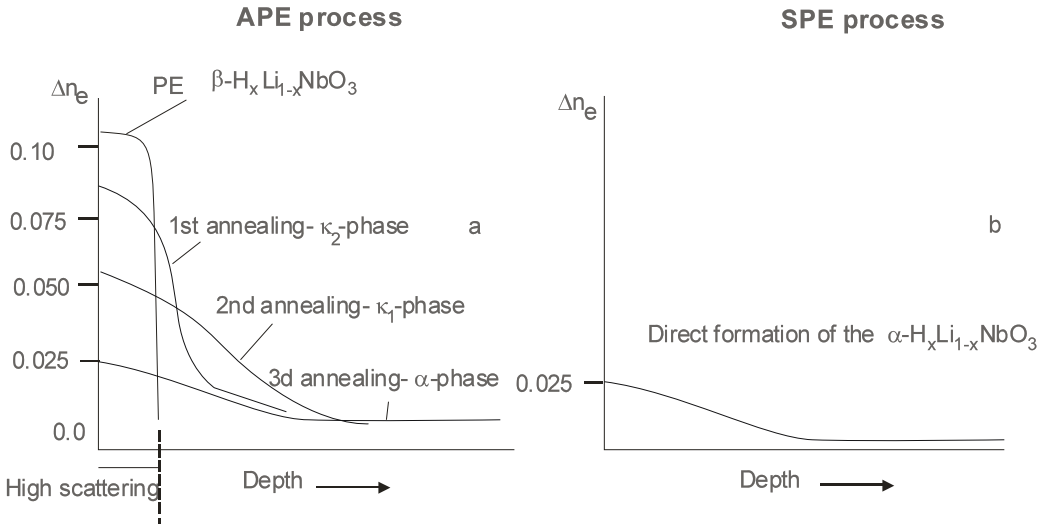

Fig.5. Formation of α-phase PE $LiNbO_3$ waveguides by APE (a) and SPE (b) processes.

With lithium stearate concentration higher than the threshold value, ρ_0, the uniform α-phase waveguides are formed. They present graded index profiles with a maximum index increase Δn_α^o=0.015 at 1550 nm wavelength.

The HTPE processes are held in specially developed containers. Specially developed metals and dielectric films are used as masks to provide the locality of proton exchange diffusion. Then, by vacuum deposition of electrodes, the integrated electro-optical phase modulators are formed on both arms of Y- splitter. Then the end surfaces are cut (the angle is 10 degree to the Y axis), polished, and finally they are coupled with anisotropic polarization holding (PANDA) fibers. The final steps are packaging and welding electrodes.

The parameters of MIOC are following:
- half wave modulation voltage: <3 V
- polarization extinction ratio: < -50dB
- intensity modulation: < 0.2%
- insertion loss (for depolarized light): < 7 dB

1.4. Block of electronics

Digital signal processor (DSP) generates voltage for "sawtooth" light modulation for compensation of Sagnac phase shift and to make fixed phase shift $\pi/2$. As a result, each channel is working in closed-loop regime. Fig.6 shows the scheme of DSP.

Analog signal from analog phase sensitive detector (PSD) that processes the output of the FOG photodetector is amplified and passed to high frequency analog to digital converter (ADC). The digital signal is demodulated by Altera Field Programmable Gate Array (FPGA). Obtained code passes to digital integrator. The signal code from integrator is used to obtain the slop of phase "saw-tooth" which corresponds to rotation rate. The Digital to Analog converter creates the analog signal from saw-tooth voltage and passes it to MIOC. The wideband integrated optic phase modulators placed at both arms of MIOC are employed to introduce phase ramp modulation, thus enabling close-loop operation. The loop

closure scheme uses a digitally synthesized saw-tooth (serrodyne modulation) of 2π amplitude in optical phase shift. In this case the Sagnac phase shift is compensated by saw-tooth modulation of light with calibrated amplitude 2π and frequency *f*, determined from well-known equation:

$$f = \frac{D}{n\lambda}\Omega$$

where Ω is a rotation rate, D – diameter of fiber coil, *n*- effective refractive index of waveguiding mode, λ - wavelength.

The frequency of resulting ramp is then a digital measure of the rotation rate, with each ramp reset proportional to the angle turned, i.e. one ramp is equal to $\frac{n\lambda}{D}$. To increase the resolution of gyro the rotation rate is determined by measuring slop of phase saw-tooth.

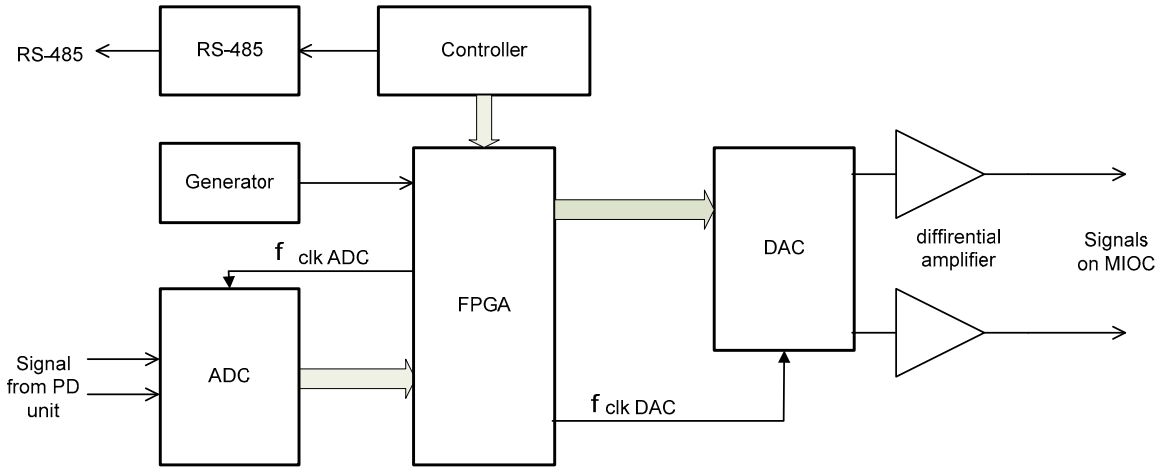

Fig.6. Block diagram of DSP.
ADC – analog digital converter, DAC – digital analog converter, FPGA – Field Programmable Gate Array, PD unit – photodetector unit.

DSP represents the circuit based on Altera's FPGA. DSP is connected with high-speed ADC and with two fast Analog Devices's DAC. Clock pulse for DAC and ADC are drawn up by FPGA. The work of FPGA is clocked by external thermo-stabilized generator.

On one of DSP the Atmel's microcontroller is established which is working as the loader for FPGA. Controller provides an exchange on interface RS-485 with external devices. The monitor for device settings is realized based on this controller. Except for loading FPGA, the controller reads out the data of measurements from FPGA.

The shaper of clock pulses transforms clock frequency to a set of impulses for synchronous work management of all devices and units. Clock frequency f_{clk} is transferred to multiple frequency AM f_{am} Clock pulses for DAC are formed on fronts AM. Clock pulses for ADC are formed so that to exclude measurements on fronts of a signal from PD.

The circuit of processing the signal coming from PD consists of the integration block, the buffer for storage of the measured value and the differencing circuit. The sum of the values of mismatch signal measured during the current phase AM is collected at the integration block. In the buffer the sum of the values measured during previous phase AM is stored. After the measurements the values from the integration block and from the buffer pass to the differencing circuit. Depending on current phase of AM, one number passes as deducted and another as the subtractor. Thus, the amplitude of a variable signal is allocated taking into account its sign.

The code with sign corresponding to a sign of a mismatch signal passes to the digital integrator, which consists of the multiplier and the summing unit with the circuit of restriction. The time constant of the digital integrator is set by the multiplier. The summing unit is used as the integrator. The code from the integrator passes to the shaper of the code for modulation compensation and then through the digital filter to the serial interface of connection with the controller.

The shaper of a code for compensating modulation includes the summing unit which forms the "saw-tooth" code and the second summing unit which is used in a contour of a digital regulator of amplitude of compensating modulation. The signal from the circuit of signal (X) processing is taken from PD at the moment of recessions of "saw-tooth". It serves as a signal of mismatch for a digital regulator of compensating modulation amplitude. The same signal is used for fine tuning of amplitude of auxiliary modulation.

There are two main sources of scale factor errors: (i) the finite flyback time and (ii) the nonstability of phase amplitude [4]. To avoid the influence of first factor we used a special transformation in the circuit that creates a control voltage signal for MIOC. In our scheme the flyback time is excluded from transmission characteristics of electro-optical modulator. The nonstability of phase amplitude is minimized by creating the astatic follow-up system. The response of device on periodic signal with calibrated constant period is considered as an error signal. Special circuit, independently on FOG moving, generates this periodic signal securing the zero error of stabilization of phase saw-tooth at 2π value at stationary rate and negligibly small error of this value at dynamic rate.

1.5. Fiber-optic gyro performance

In our design we reduced the fundamental limitation of FOG performance as much as possible [8]:

Optical losses

Sensitivity of IFOG is limited by shot noise that goes as the square root of the power, which decreases with fiber length. However, the Sagnac effect increases with the length of the fiber. These two competing effects set the length of the fiber for a given sensitivity.

Thermal Noise

Time dependent temperature gradient along the length of the fiber can introduce spurious phase shifts due to the temperature dependence of the refractive index of fiber. To minimize this effect the fibers with smaller dn/dT dependence should be used. Also, quadropole winding such that equidistant points from fiber center are physically close to each other strongly reduces this effect.

Backscattering of light

Backscattered light at the output-input couplers and MIOC facets can interfere with the main beams creating parasitic interference effects. Immersion cells that reduce refraction index step, as well as the use of tilted MIOC facets reduce backscattering.

Optical Kerr Effect

Electric fields of the counter-propagating beams can cause changes in the as much as possible index that is nonreciprocal if the light is split into inequal parts. The nonreciprocity induced by the nonlinear Kerr effect can be strongly reduced by using broad-band, low coherence, unpolarized optical sources or even with a simple 50% duty cycle modulation of the input optical power.

Magneto-optical effect

The magneto-optical Faraday effect is a nonreciprocal effect which is potentially dangerous in adding to the Sagnac effect. This problem is now almost solved by the use of carefully untwisted polarization maintaining fibers as well as by using cases from special materials (permalloy, etc.)

For the IFOG with perfect components (ideal splitter, no backscattering, etc.), the measurement limit is imposed by the shot noise in the light measured by photodetector. The uncertainty $\delta\Omega_\pi$, generated by the fluctuation in the light due to shot noise can be expressed as [6]:

$$\delta\Omega_\pi = \frac{c}{L \cdot D} \frac{\lambda / 2}{\left(n_p n_D \tau\right)^{\frac{1}{2}}}$$

where n_p is the number of photons per second coming to photodetector, n_D is detector quantum efficiency and τ is averaging time

The main parameters of produced and commercially available Optolink's FOGs are presented at Table 2.

Table 2. Parameters of Optolink's fiber-optic gyroscopes.

Parameter	Single axis SRS-2000	Single axis SRS-1000	Single axis SRS-501	Three axes TRS-500	Single axis SRS-200
Range of measured angular rate, deg/sec	±40	±90	±250	±300	±600
Bias drift at fixed temperature, deg/h	0.005	0.01	0.1	0.1	0.2
Bias drift at changing temperature from -40°C till 60°C, deg/h	0.02	0.05	0.5	0.5	0.5
Scale factor repeatability, %:	0.003	0.005	0.05	0.07	0.05
Bandwidth, Hz:	50	100	300	300	400
Random walk, deg/√h	0.0003	0.0005	0.009	0.02	0.02
Power supply, V:	5 ± 0.25	5 ± 0.25	5 ± 0.25	5 ± 0.25	5 ± 0.25
Power consumption, W:	<6	<6	< 6	<6	< 5
Weight, kg	1.1	0.8	0.35	1.2	0.22
Dimensions, mm:	Ø 250x80	Ø150x80	Ø100x30	110x110x90	Ø70x28
Output:	RS485/422	RS485/422	RS485/422	RS485/422	RS485/422

REFERENCES

[1] Lefevre, H., [The Fiber Optic Gyroscope], Artech House, (1993).

[2] Korkishko, Y.N., Fedorov, V.A., and Feoktistova, O.Y., "$LiNbO_3$ optical waveguide fabrication by high-temperature proton-exchange", IEEE J. Lightwave Technol., 18, 562-568, (2000).

[3] [Optical Gyros and their Application], RTO – AG, 339, (1999).

[4] Suchoski, P.G., Findakly, T.K., and Leonberger, F.J., "Stable low-loss proton-exchanged $LiNbO_3$ devices with no electro-optic degradation", Opt. Lett., 13, 1050-1052, (1988).

[5] Korkishko, Yu.N., and Fedorov, V.A., "Structural Phase Diagramm of $H_xLi_{1-x}NbO_3$ waveguides: The Correlation Between Structural and Optical Properties", IEEE Journal of Selected Topics in Quantum Electronics, 2, 2, 187-196, (1996).

[6] Davis J.L., Ezekiel S. , Proc.SPIE,, 157, 131-137, (1978).